

Ratiometric Fluorescent Detection of Phosgene in Liquid and Gas Phases Using a Tautomeric Dye: A Combined Experimental and Theoretical Study

Afna Ummer^{a,b}, Avijit Kumar Das^{*a,b}, Malavika S Kumar^{a,b}, Urmila Saha^c, Malay Dolai^{d*}

^a Department of Chemistry, Christ University, Hosur Road, Bangalore, Karnataka, 560029
India

*Email: avijitkumar.das@christuniversity.in; sanjuavi.das@gmail.com

^b Centre for Renewable Energy and Environmental Sustainability, Christ University,
Karnataka, 560029, India

^c Department of Chemistry, Indian Association for the Cultivation of Science, Raja SC Mullick
Road, Kolkata 700032, WB, India

^d Department of Chemistry, Prabhat Kumar College (Vidyasagar University), Purba Medinipur
721404, WB, India. E-mail: dolaimalay@yahoo.in

CONTENTS

- 1. Preparation of phosgene gas**
- 2. General methods of UV-*vis* and fluorescence titration experiments**
- 3. Calculation of the detection limit**
- 4. Rate constant calculation**
- 5. Stern-Volmer plot**
- 6. NMR spectra**
- 7. Mass spectra**
- 8. Computational Analysis**
- 9. References**

1. Preparation of phosgene gas

As phosgene is toxic, volatile and difficult in handling hence, during the experiments we use less toxic, non-volatile Tri phosgene ($\text{CCl}_3\text{OC(O)OCCl}_3$) as the precursor of phosgene gas. It generates phosgene gas in presence of triethylamine (TEA). In all the experiments acetonitrile has been used as solvent.

2. General method of UV-*vis* and fluorescence titration:

By UV-*vis* method:

For UV-*vis* titrations, stock solution of the sensor was prepared ($c = 2 \times 10^{-5}$ M) in CH_3CN . Tri phosgene solution of concentration ($c = 2 \times 10^{-4}$ M) was prepared in CH_3CN and triethylamine was added to the solution (1:5 molar ratio). The solution of the guest interfering analytes like CH_3COOH , $\text{C}_4\text{H}_9\text{F}$, $\text{C}_4\text{H}_9\text{Br}$, $\text{C}_4\text{H}_9\text{I}$, CH_3COCl , $\text{C}_6\text{H}_5\text{COCl}$, $\text{C}_6\text{H}_5\text{CH}_2\text{Cl}$, SOCl_2 , $\text{C}_7\text{H}_7\text{SO}_2\text{Cl}$, and COCl_2 were also prepared in the order of ($c = 2 \times 10^{-4}$ M). Initially sensor **HHP** solution was prepared by dissolving the sensor in 2 ml acetonitrile followed by the gradual addition of corresponding guest analytes with the particular concentration. Solutions of various concentrations containing sensor and increasing concentrations of analytes were prepared separately. The spectra of these solutions were recorded by means of UV-*vis* methods.

By fluorescence method:

For fluorescence titrations, stock solution of the sensor ($c = 2 \times 10^{-5}$ M) was prepared for the titration of analytes in CH_3CN . Initially sensor **HHP** solution was prepared by dissolving the sensor in 2 ml acetonitrile followed by the gradual addition of corresponding guest analytes with the particular concentration. The solution of the guest analytes in the order of 2×10^{-4} M was also prepared. Solutions of various concentrations containing sensor and increasing concentrations of analytes were prepared separately. The spectra of these solutions were recorded by means of fluorescence methods.

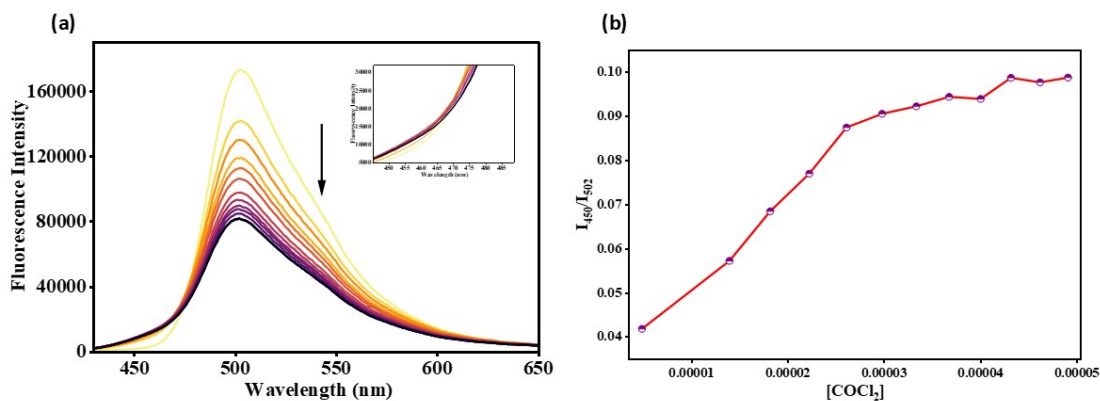


Figure S1. (a) Fluorescence titration spectra of **HHP** ($c = 2.0 \times 10^{-5}$ M) with phosgene ($c = 2.0 \times 10^{-4}$ M). (b) The variations in emission intensity with respect to phosgene concentration at wavelength ratio I_{450}/I_{502} .

3. Calculation of the detection limit:

The detection limit DL of **HHP** for phosgene was determined from the following equation: $DL = K \cdot Sb1/S$ Where $K = 2$ or 3 (we take 3 in this case); $Sb1$ is the standard deviation of the blank solution; S is the slope of the calibration curve. From the graph Fig.S1, we get slope = 147059 , and $Sb1$ value is 2384.91 . Thus, using the formula, we get the Detection Limit for phosgene = $3.82 \mu\text{M}$.

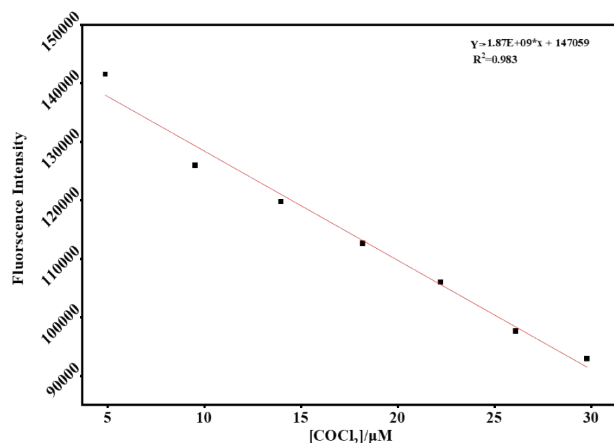


Figure S2. Changes of fluorescence Intensity of **HHP** as a function of $[\text{COCl}_2]$

4. The changes of emission curve of **HHP** ($c = 2 \times 10^{-5}$ M) at different time interval by addition of phosgene ($c = 2 \times 10^{-4}$) and calculation of first order rate constant:

Fig.S2 represents the changes of emission intensity at different time interval by addition of triphosgene/TEA. From the time vs. fluorescent intensity plot at fixed wavelength at 502 nm

by using first order rate equation we get the rate constant $K = \text{slope} \times 2.303 = 159.61 \times 2.303 = 367.58 \text{ sec}^{-1}$.

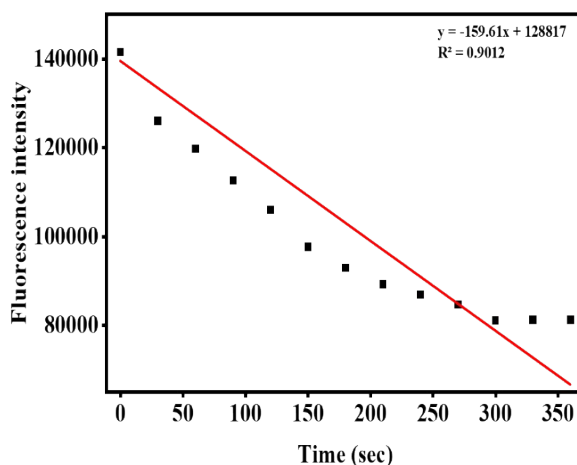


Figure S3. The first order rate equation by using time vs. fluorescence intensity plot at 502 nm.

5. Stern- Volmer plot

The quenching efficiency and sensitivity were evaluated by calculating the Stern–Volmer quenching constant (K_{SV}), calculated by the Stern–Volmer (SV) equation: $I_0/I = 1 + K_{SV}[COCl_2]$, where K_{SV} is the quenching constant (M^{-1}), I_0 and I are the fluorescence intensities of complexes before and after the addition of phosgene, and $[COCl_2]$ is the molar concentration of phosgene.

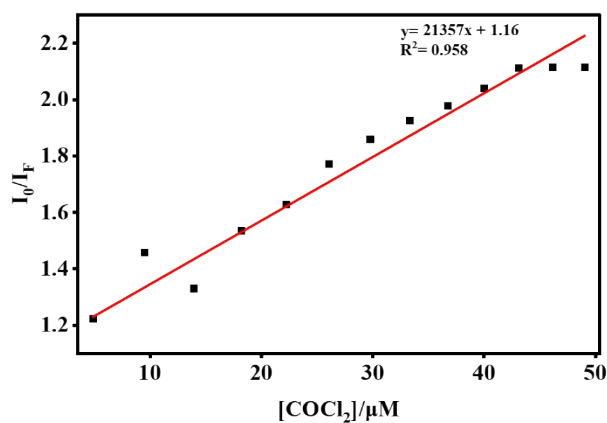


Figure S4. Stern Volmer quenching constant of **HHP** with the concentration of phosgene vs changes of fluorescence intensity.

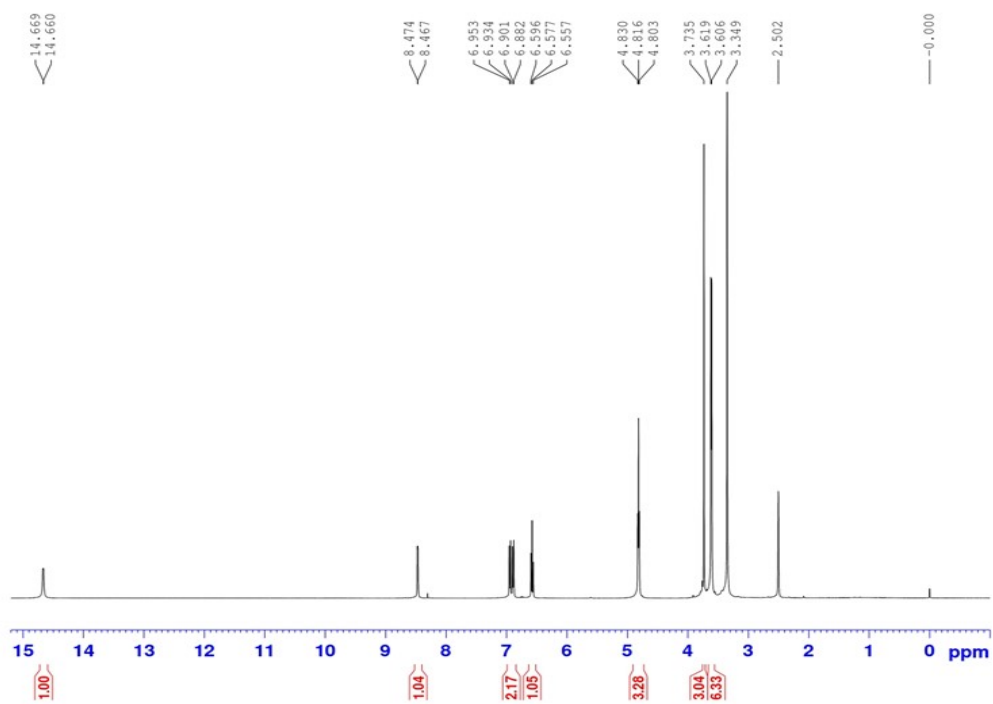
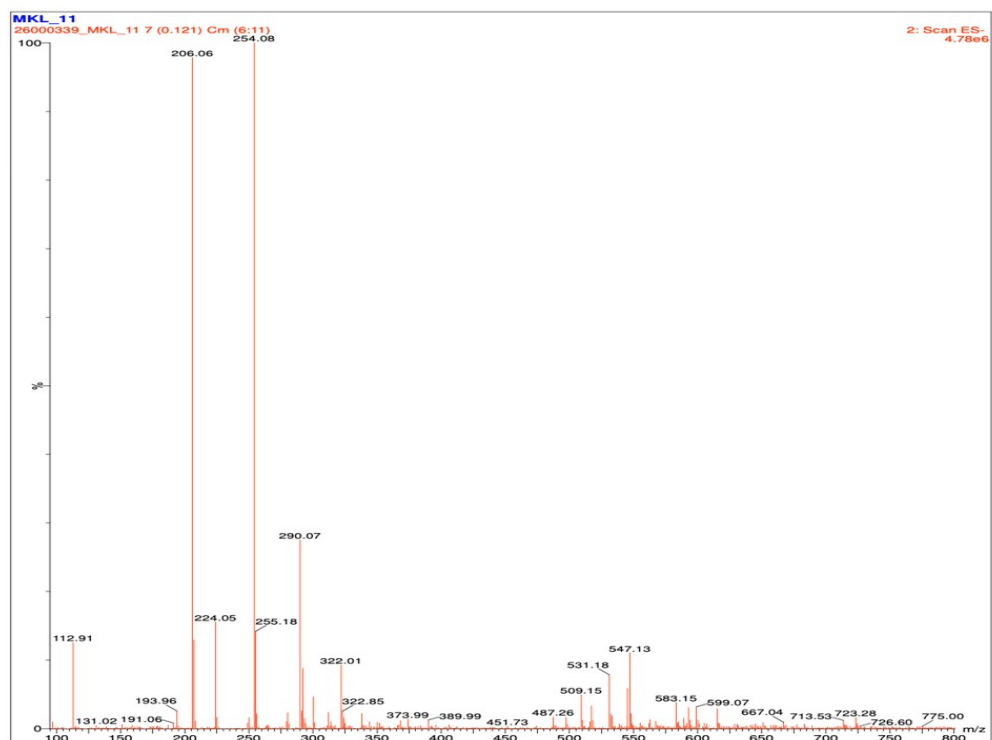


Figure S5. $^1\text{H-NMR}$ spectra of **HHP** in DMSO-d_6

(a)



(b)

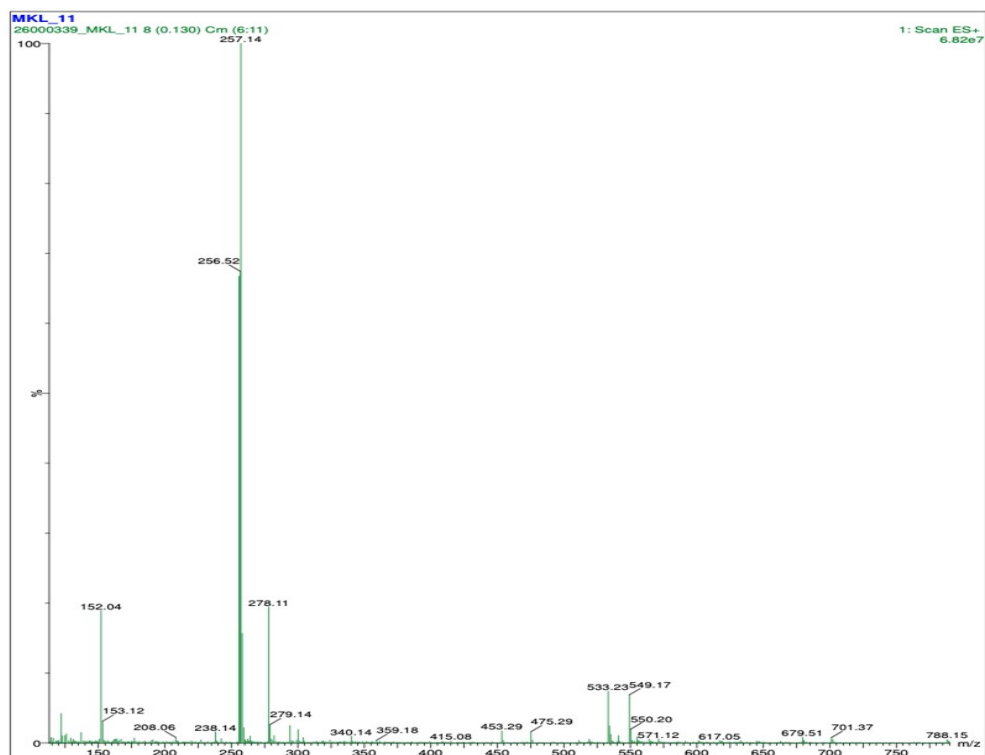


Figure S6. Mass spectra of HHP: (a) Negative mode; (b) Positive mode.

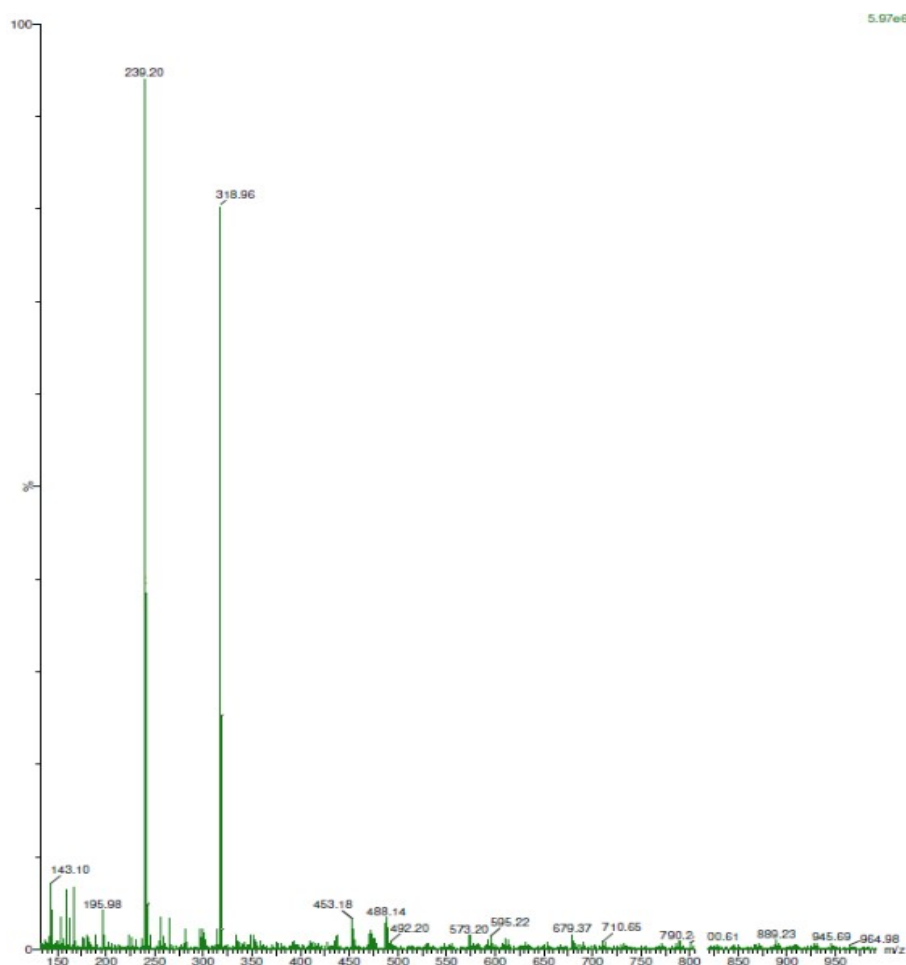


Figure S7. Mass spectra of **HHP** and phosgene complex (**HHP-P**)

6. Computational details

Methods for DFT

Density Functional Theory (DFT)¹ calculations were conducted using the Gaussian 09 (Revision A.02) package, with "Gauss View" utilized for visualizing molecular orbitals. Becke's three-parameter hybrid-exchange functional, the Lee-Yang-Parr expression for nonlocal correlation, and the Vosko-Wilk-Nuair 1980 local correlation functional (B3LYP) were employed in the calculation.²

Optimization of **HHP** and **HHP-P** with the single-point energy calculations in the gas phase were performed using the 6-31+(g) basis set. For C, N, O and H atoms we used 6-31+(g) basis set. The calculated electron-density plots for frontier molecular orbitals were prepared by using Gauss View 5.1 software. All the calculations were performed with the Gaussian 09W software package.³

7. References:

1. R. G. Parr and W. Yang, *Density Functional Theory of Atoms and Molecules*, Oxford University Press, Oxford, 1989.
2. (a) A. D. Becke, *J. Chem. Phys.*, 1993, 98, 5648. (b) C. Lee, W. Yang and R. G. Parr, *Phys. Rev. B*, 1998, 37, 785.
3. M. J. Frisch, G. W. Trucks, H. B. Schlegel, G. E. Scuseria, M. A. Robb, J. R. Cheeseman, G. Scalmani, V. Barone, B. Mennucci, G. A. Petersson, H. Nakatsuji, M. Caricato, X. Li, H. P. Hratchian, A. F. Izmaylov, J. Bloino, G. Zheng, J. L. Sonnenberg, M. Hada, M. Ehara, K. Toyota, R. Fukuda, J. Hasegawa, M. Ishida, T. Nakajima, Y. Honda, O. Kitao, H. Nakai, T. Vreven, J. A. Montgomery Jr., J. E. Peralta, F. Ogliaro, M. Bearpark, J. J. Heyd, E. Brothers, K. N. Kudin, V. N. Staroverov, R. Kobayashi, J. Normand, K. Raghavachari, A. Rendell, J. C. Burant, S. S. Iyengar, J. Tomasi, M. Cossi, N. Rega, J. M. Millam, M. Klene, J. E. Knox, J. B. Cross, V. Bakken, C. Adamo, J. Jaramillo, R. Gomperts, R. E. Stratmann, O. Yazyev, A. J. Austin, R. Cammi, C. Pomelli, J. W. Ochterski, R. L. Martin, K. Morokuma, V. G. Zakrzewski, G. A. Voth, P. Salvador, J. J. Dannenberg, S. Dapprich, A. D. Daniels, Ö. Farkas, J. B. Foresman, J. V. Ortiz, J. Cioslowski and D. J. Fox, *Gaussian Inc.*, 2009, Wallingford CT.